Iraqi Journal of Science, 2026, Vol. xx, No. x, pp: xx
DOI: 10.24996/ijs.2026.67.1.17

ISSN: 0067-2904

Green Synthesis of Iron Oxide Nanoparticles and its Application in Polluted Water Treatment

Zainab Saad Mahdi[1*], Intesar H. Hashim[1], Nadia M. Jassim[2]
[1]*Department of Physics, College of Education, Mustansiriyah University, Baghdad-Iraq*
[2]*Department of Physics, College of Science, University of Diyala, Diyala- Iraq.*

Received: 11/7/2024 Accepted: 16/1/2025 Published: xx

Abstract

The green synthesis of nanomaterials is of particular interest to researchers worldwide. It is described as a simple, robust, inexpensive, and environmentally friendly method. This research presented an easy and quick method to biosynthesize iron oxide nanoparticles (Fe_3O_4NPs) using hibiscus flower extract. The biosynthesized Fe_3O_4NPs were used to treat polluted water samples taken from different points on the Euphrates River in Iraq. The nanoparticles were characterized using X-ray diffraction (XRD), energy dispersive X-ray spectroscopy (EDX), field emission scanning electron microscopy (FE-SEM), atomic force microscopy (AFM), Fourier transform infrared spectroscopy (FTIR), the surface-enhanced Raman scattering (SERS) and ultraviolet-visible (UV-Vis) spectroscopy. The use of magnetic adsorbents, especially (Fe_3O_4) is a promising adsorbent for water purification due to its high surface area. Its superior magnetism and ease of operation make it suitable for absorbing many pollutants, as well as its biological effectiveness against gram-negative bacterial strains that are usually found in polluted water (*Pseudomonas, Acinetobacter, Cholera, and Escherichia coli*).

Keywords: Green synthesis, Fe_3O_4 NPs, Polluted water treatment, Adsorbents, *Escherichia coli.*

التوليف الأخضر لجسيمات أكسيد الحديد النانوية وتطبيقاتها في معالجة المياه الملوثة

زينب سعد مهدي [1*], انتصار هاتوهاشم[1], نادية محمد جاسم[2]
[1]قسم الفيزياء, كلية التربية، الجامعة المستنصرية, بغداد، العراق
[2]قسم الفيزياء, كلية العلوم, جامعة ديالى, ديالى، العراق.

الخلاصة

يعد التوليف الأخضر للمواد النانوية ذا أهمية خاصة للباحثين في جميع أنحاء العالم. وتوصف بأنها طريقة بسيطة وقوية وغير مكلفة وصديقة للبيئة. قدم هذا البحث طريقة سهلة وسريعة لتصنيع جسيمات الحديد النانوية المؤكسدة حيوياً (Fe_3O_4NPs)باستخدام مستخلص زهرة الكركديه، ومن ثم تم استخدام Fe_3O_4NPs المحضر حيوياً لمعالجة عينات المياه الملوثة المأخوذة من نقاط مختلفة على نهر الفرات في العراق. تم تشخيص الجسيمات النانوية باستخدام حيود الأشعة السينية (XRD), التحليل الطيفي للأشعة السينية المشتتة من الطاقة (EDX) , مجهر مسح إلكتروني بانبعاث المجال (FE-SEM) , مجهر القوة الذرية (AFM) , مطيافية تحويل فوريه بالأشعة تحت الحمراء (FTIR), تشتت رامان المعزز على السطح (SERS) ومطيافية الأشعة فوق البنفسجية المرئية (UV-vis). يعد استخدام الممتزات المغناطيسية وخاصة (Fe_3O_4) من المواد الممتزة الواعدة لتنقية

*Email: zainab.saad@uodiyala.edu.iq

المياه بسبب مساحة سطحها العالية. مغناطيسيتها الفائقة وسهولة تشغيلها تجعلها مناسبة لامتصاص العديد من الملوثات، فضلاً عن فعاليتها البيولوجية ضد السلالات البكتيرية سالبة الجرام التي توجد عادة في المياه الملوثة (*Pseudomonas, Acinetobacteria, Cholera, and Escherichia coli*).

1. Introduction

Nanotechnology is a branch of applied science and technology whose interest is controlling matter at the nanoscale, extending from 1 to 100 nanometers [1]. Nanomaterials are classified into many groups based on their size, shape, and physical and chemical properties [2]. Magnetic nanoparticles (MNPs) are among the most essential nanomaterials and have many practical applications, such as magnetic fluids, biosensors, catalysts, separation processes, and environmental remediation [3]. Although many iron oxides are known, the term "iron oxides" usually refers to three types: Fe_3O_4 (magnetite), $\gamma - Fe_2O_3$ (maghemite), and $\alpha - Fe_2O_3$ (hematite) [4]. Fe_3O_4 nanoparticles can be prepared by traditional physical and chemical methods, which may be expensive, environmentally pollutant, and time-consuming, so it is preferable to prepare it in a simple, safe, low-cost, and environmentally friendly method, such as the green synthesis method that increases the colloidal stability of material, in addition to the physical and chemical properties of Fe_3O_4 synthesized by this method. It can exhibit better water permeability, antioxidant activity, biocompatibility, biodegradability, and acceptable toxicity for various biomedical applications compared with using other traditional methods [5]. This study prepared Fe_3O_4 nanoparticles by the green synthesis method using the hibiscus flower. With their promising properties, these nanoparticles were used to treat polluted water at different points of the Euphrates River, offering a glimpse into the future of water treatment. This is done by improving water quality by removing pollutants and unwanted components to become suitable for the desired end-use. Since rivers are the primary sources of water for various uses as well as the primary sources of pollution through the major cities located on them and industrial activities, river water is polluted with physical and biological impurities, such as total suspended solids, bacteria, viruses, algae, etc. [6], which must be removed through different treatment processes. The water parameters, such as pH, electrical conductivity, total hardness, total solids, and total suspended salts, were measured if higher or lower after treatment to determine the quality and effectiveness of treatment [7].

2. Experimental Part

2.1 Sample Preparation

Polluted samples of water from the Euphrates River at different points were collected. The samples included factory waste (Diwaniaya factory for tiers near Euphrates River) and sewage water. The chemical, physical, and biological properties of all collected samples were studied. The chemical properties included pH, total dissolved salts (TDS), total suspended solids (TSS), and total hardness (TH). Physical properties included the electrical conductivity (E.C) and turbidity (Turb). Meanwhile, the biological category was represented by aerobic bacterial total (T.P.C). All measured parameters of collected samples were compared to those of the sterile water. All measurements were done in the Department of Environment Laboratories in Diyala Governorate.

2.2. Preparation of Iron Oxides Nanoparticles

Nano-iron oxides (Fe_3O_4) were prepared using the hibiscus flower's green synthesis method. The hibiscus flowers were ground and sieved using a 38 μm diameter micro sieve. Then, 2 gm of the hibiscus powder was added to 100 ml of deionized water, and the solution was placed on a magnetic stirrer at 50 °C for an hour until the color of the solution turned dark red. An hour after preparing the solution, it was filtered. 0.82 gm of iron chloride at a concentration of 0.5 mM was mixed with 100 ml of deionized water; then, the solution was placed on a magnetic

stirrer at 50 ºC for an hour until the chloride dissolved completely. The color of the solution became bright golden yellow. To prepare iron oxide nanoparticles, 10 ml of the hibiscus solution was added drop by drop to the iron chloride solution and placed on a magnetic stirrer for an hour until the color of the solution became dark brown, as shown in Figure 1; the formation of iron oxide indicated in Equation 1. Iron oxide nanoparticles were characterized using various analytical techniques, including X-ray diffraction (XRD) (PAN analytical Aeris X-ray diffractometer) (Cu Kα1 radiation and wavelength of 1.54059 Å), Energy Dispersive X-ray spectroscopy (EDX) (TESCAN, Mira3, Czech Republic), Atomic Force Microscopy (AFM)(Model TT-2), Field Emission Scanning Electron microscopy (FE-SEM)(inspect TM F50), Fourier Transform Infrared Spectroscopy (FTIR) (Model Spectrum Two Perkin Elmer), Raman Spectroscopy(Teksan, TakRam N1-541, Iran) and UV-Vis spectroscopy.

$$3FeCl_3 + Reducing\ agent\ (from\ hibiscus) + 8OH \longrightarrow Fe_3O_4 + 9Cl - + 4H_2O \quad \ldots\ldots\ldots\ldots\ldots (1)$$

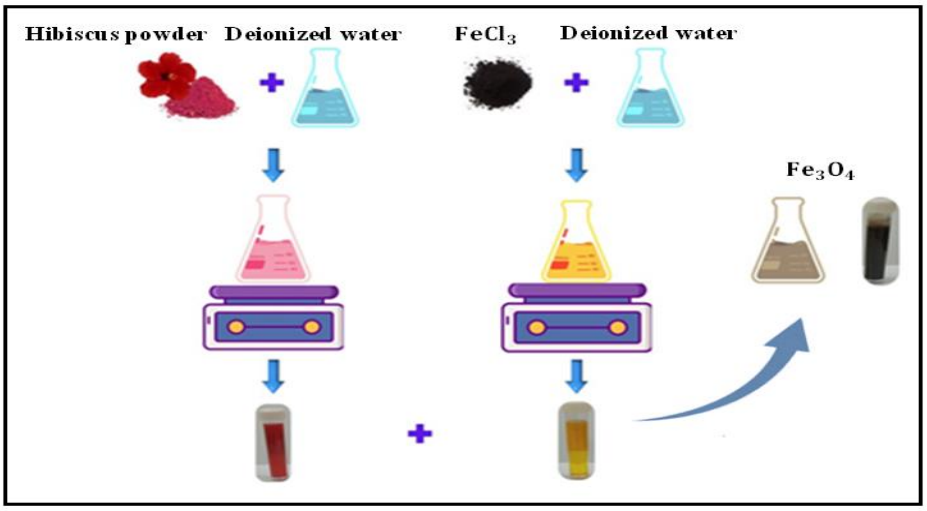

Figure 1: Schematic diagram of the synthesis process of Fe_3O_4NPs.

2.2.2. Treatment by Fe_3O_4NPs

1 ml of Fe_3O_4NPs was added to 100 ml of the collected water samples and placed on an ultrasonic device for one hour at room temperature. The samples were left in the ultrasound machine for 4-6 hours; they were left until the added nanoparticles settled at the bottom of the beaker (stagnant); afterward, the water was filtered using filter paper. The physical and chemical properties of the samples were tested after the treatment process.

2.2.3. Biological Application

The antibacterial ability of Fe_3O_4NPs against gram-negative bacterial strains, usually found in polluted water (*Pseudomonas, Acinetobacteria*, *Cholera*, and *Escherichia coli*), was studied using agar diffusion assay [8, 9]. About 20 ml of Mueller-Hinton (MH) agar was aseptically poured into sterile Petri dishes. Bacterial species were collected from their cultures using a sterile wire loop [10]. After culturing the organisms, 6-mm diameter wells were drilled onto the agar plates using a sterile tip. In the drilled wells, different concentrations of samples Fe_3O_4NPs were placed. The culture plates containing the Fe_3O_4NPs and test organisms were incubated for 24 hours at 37°C before measuring and recording the average diameter of inhibition zones [11, 12].

3. Results and Discussion

3.1. Structural and Morphological Properties

Iron oxide nanoparticles were prepared using the green synthesis technique for use in contaminated water treatment. XRD, AFM, and FE-SEM determined their structural and morphological properties. XRD results indicated that the Fe_3O_4NPs are polycrystalline; the XRD pattern of Fe_3O_4NPs showed peaks in the dominant direction (220), (400), (422), (440), and (533), which correspond to the crystal planes of pure cubic spinel crystal structure phase of Fe_3O_4 standard card data (JCPDS file number: 00-003-0863) [13, 14], as shown in Figure 2. The crystallite size was calculated using the well-known Scherrer equation ($D_{hkl} = K\lambda/(B_{hkl}cos\theta)$). Table 1 shows the X-ray diffraction parameters of the prepared Fe_3O_4NPs.

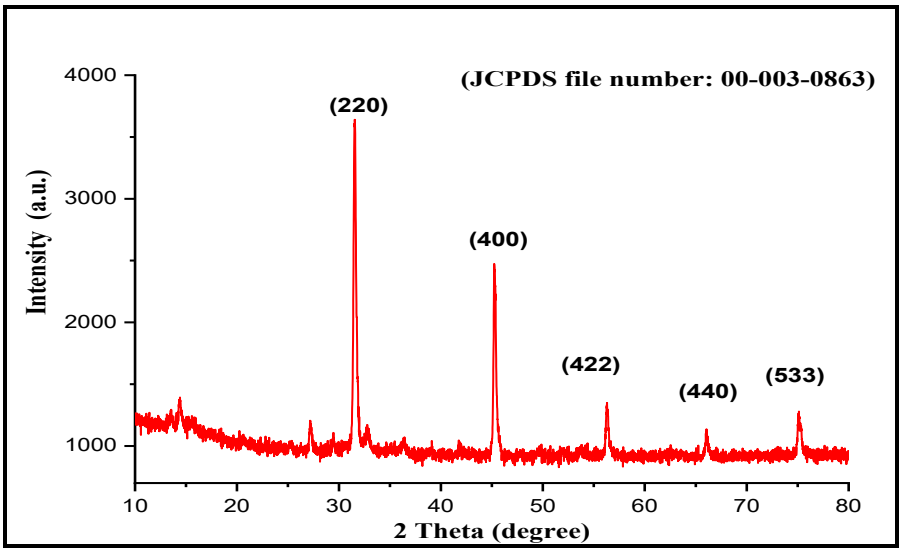

Figure 2: XRD pattern of Fe_3O_4NPs.

Table 1 : Fe_3O_4 NPs XRD measurements

NO.	2θ	Intensity	Crystalline size (nm)
1	15.9008	6.53	56.3
2	20.8457	6	44.1
3	27.2383	10.59	81.5
4	29.4057	1.78	18.0
5	31.5992	100	226.3
6	42.6316	2.54	38.2
7	45.3374	69.9	566.7
8	45.484	31.7	3033.8
9	49.6158	6.56	71.7
10	56.3696	17.88	3166.5
11	66.1233	4.57	80.4
12	75.1942	9.43	132.1

The surface topography of the synthesized Fe_3O_4NPs was investigated with AFM images, which provide a three-dimensional surface profile of the synthesized Fe_3O_4NPs, as shown in Figure 3-A; the height measurements in the AFM images can give the height of nanoparticles with high accuracy. Fineness refers to an average grain size of 14.47 nm, average roughness of 32.90 nm, and root mean square of 2.99 nm, as shown in Table 2. Figure 3-B shows the size

distribution of magnetic Fe_3O_4NPs between 75 and 90 nm. This result agrees with that of Gnanasekar et al. [15].

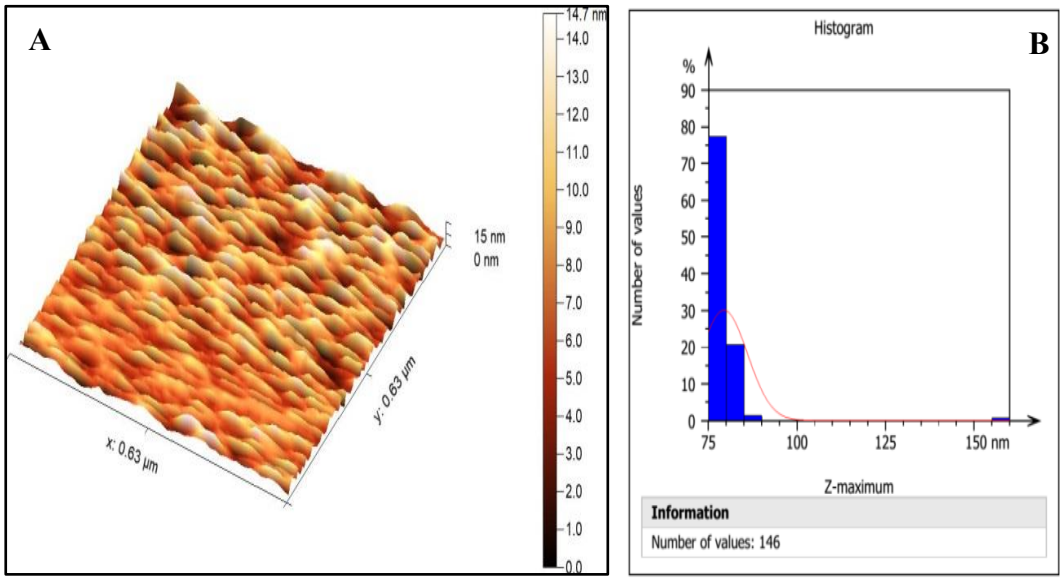

Figure 3: 3DAFM images of Fe_3O_4NPs (A) the height measurements and (B) the size distribution of magnetic Fe_3O_4NPs

Table 2: AFM Results of Fe_3O_4 NPs

Samples	Average grain size (nm)	Roughness average (nm)	Root Mean Square (nm)
Fe_3O_4	14.47	32.90	2.99

Field Emission Scanning Electron Microscope (FE-SEM) analysis was used to characterize the shape and size of the Fe_3O_4NPs. The nanoparticles were in sizes ranging from 58.48 nm to 97.14 nm, as shown in Figure 4; it was found that the average particle size of iron oxide particles was 78.12 nm, with a spherical shape. This result is in agreement with Mostafa et al. results[16].

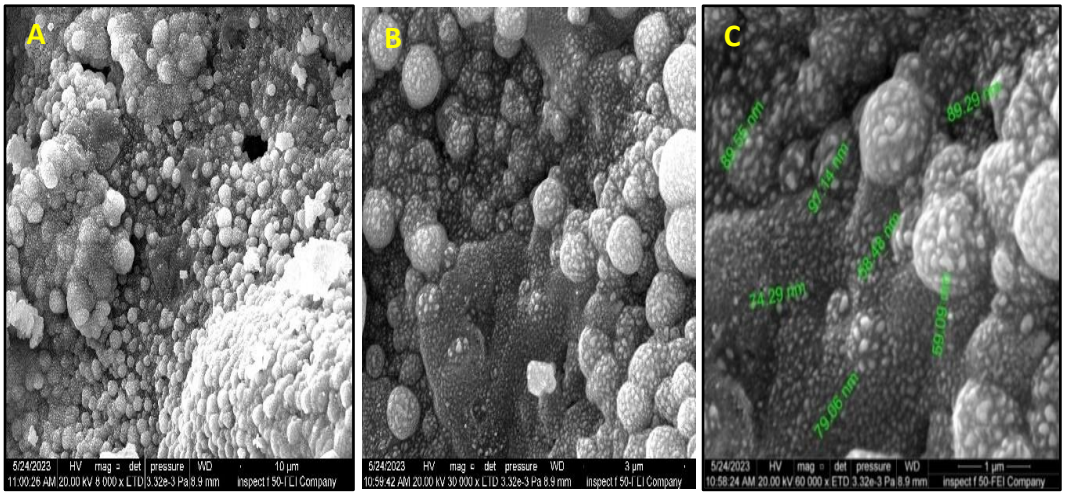

Figure 4: FE-SEM images of Fe_3O_4NPs measurement at range (A) 10 µm (B) 5 µm (C) 1 µm

4.2. Energy Dispersive X-ray Spectroscopy

Energy Dispersive X-ray spectroscopy (EDX) was used to identify elements present in the water samples taken from factory waste and wastewater flowing into the Euphrates River before and after treatment with Fe_3O_4NPs. It was noted that the sodium element in the factory waste sample decreased after treatment, while its percentage increased in the sewage waste sample after treatment. This is the same behavior as the chlorine element in both samples. Calcium was observed to appear in the factory waste sample after treatment; its percentage in the sewage waste sample decreased. While the rate of oxygen increased after treatment in both samples. Finally, it was noted that the factory waste sample does not contain sulfur, but in the sewage waste sample, the sulfur element disappears after being treated with iron oxide, as shown in Figure 5, Table 3.

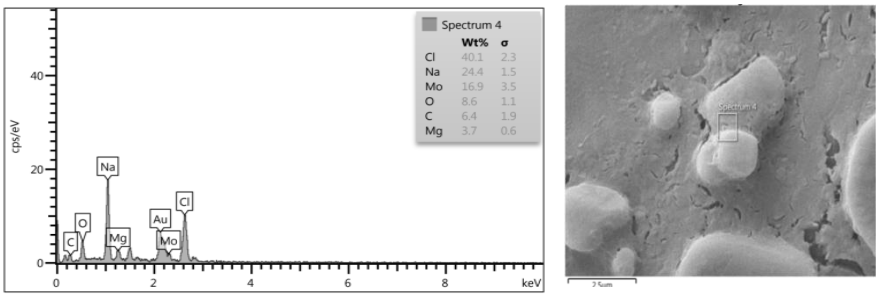

A- Before Treatment

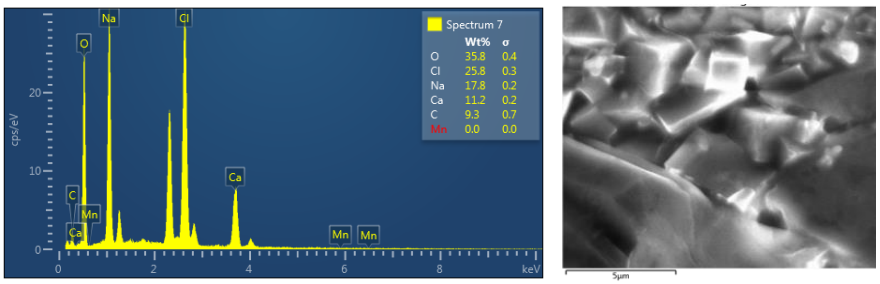

A- After Treatment by Fe_3O_4 NPs

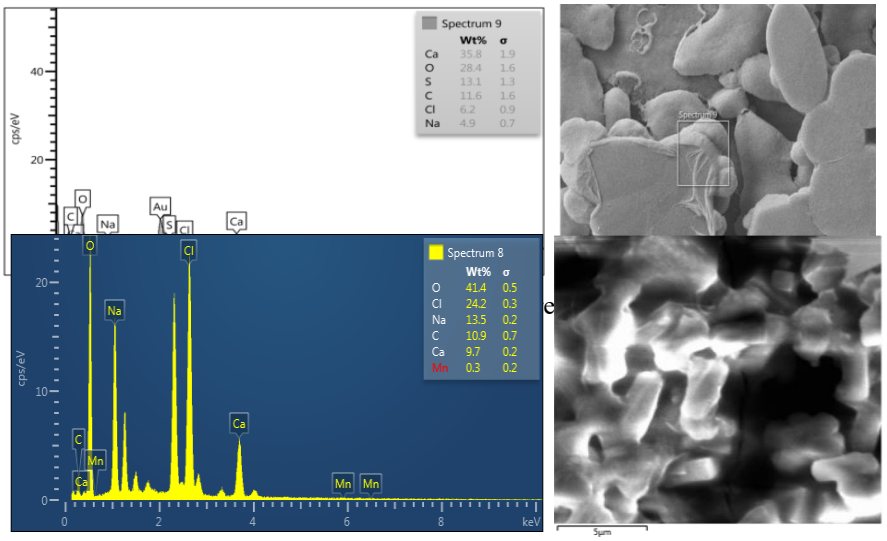

B- After Treatment by Fe_3O_4 NPs

Figure 5: EDX of Euphrates River samples before and after treatment for A-factory waste and B-Sewage water.

Table 3: EDX Results of water samples from Euphrates River

Sample	Treatment	Elements Ratio Wt %						
		S	O	Na	C	Ca	Mg	Cl
A -Factory waste	Before	-	8.6	24.4	6.4	-	3.7	40.1
	Fe_3O_4NPs	-	35.8	17.8	9.3	11.2	-	25.8
B - Sewage water	Before	13.1	28.4	49	11.6	35.8	-	6.2
	Fe_3O_4NPs	-	41.4	13.5	10.9	9.7	-	24.12
Sterile water		-	7.3	-	-	81.1	-	-

4.3 FTIR Results of Fe_3O_4 NPs

The functional groups in Fe_3O_4 NPs have been mapped using FTIR spectroscopy; in the FTIR spectrum, as shown in Figure 6. The Fe_3O_4 spectra were recorded in the range (721.49-3436.92 cm^{-1}). Several significant absorption peaks can be observed. The infrared spectrum of Fe_3O_4 NPs shows broad absorption bands at (3436.92 cm^{-1}), which corresponds to the O-H stretching bands attributed to compound alcohols [17], at (2954.51, 2924.17, 1383.35 cm^{-1}) corresponding to C-H alkenes [16], [17], respectively, at (2854.21 cm^{-1}), which corresponds to C-H compound amides [16], at (1636.94 cm^{-1}) which corresponds to C=O groups function carboxyl [17], at (1099.97,1075.13,1031 cm^{-1}) which corresponds to C-O groups function carboxylic acids [16], and at (721.49 cm^{-1}) which corresponds to Fe-O groups function metal oxide [16]. Table 4 shows FTIR measurements, which indicates that the transmittance is a function of the wavenumber.

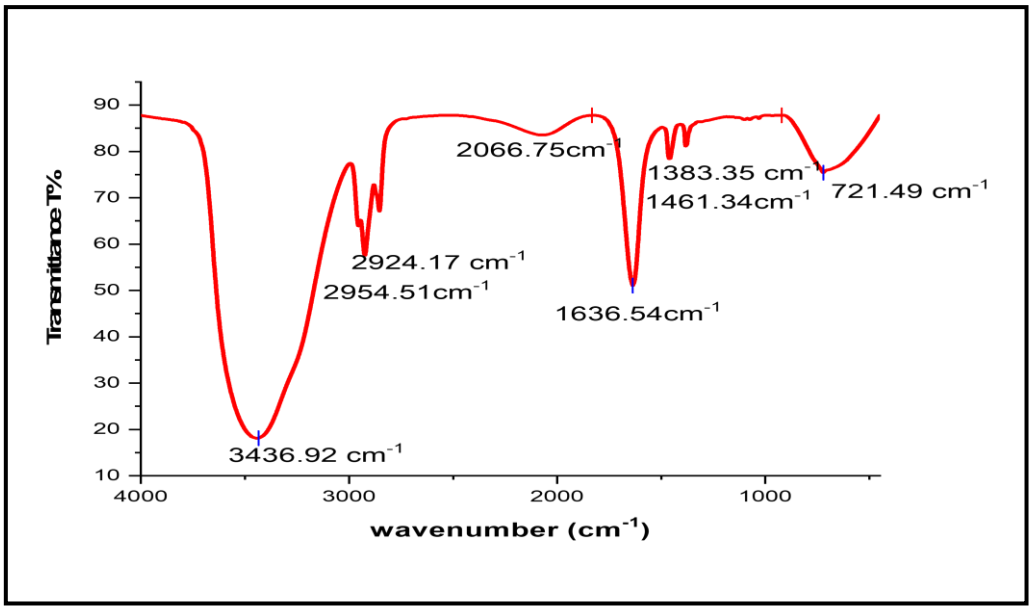

Figure 6: FTIR of Fe_3O_4NPs

Table 4 : FTIR measurement results

Peak Number	Wavenumber (cm^{-1})	Transmittance (a.u.)	Group	Compound Class
1	3436.92	18.12	O-H	alcohol
2	2954.51	63.90	C-H	alkene
3	2924.17	57.57	C-H	alkene
4	2854.21	67.11	C-H	amides
5	2066.75	83.53	C-H	aromatic compound
6	1636.94	51.03	C=O	carboxyl
7	1461.34	78.42	C=O	carboxyl
8	1383.35	81.12	C-H	alkene
9	1099.97	86.84	C-O	carboxylic acids
10	1075.13	86.84	C-O	carboxylic acids
11	1031.00	87.08	C-O	carboxylic acids
12	721.49	75.40	Fe-O	metal oxide

Raman spectroscopy gives information on the vibrations of the bonds present in the analyzed material, giving evidence of the material's chemical composition and structure [18]. Figure 7 shows the Raman spectra in the range of 668.75 cm^{-1} to 3236.29 cm^{-1} of water samples taken from different locations of the Euphrates River. The Raman intensity decreased after treatment, meaning the concentration of materials decreased [19]. Compared with the vibrations recorded in previous studies and some references, these vibrations describe the vibrations of water molecules and other material components [19], as shown in Table 5.

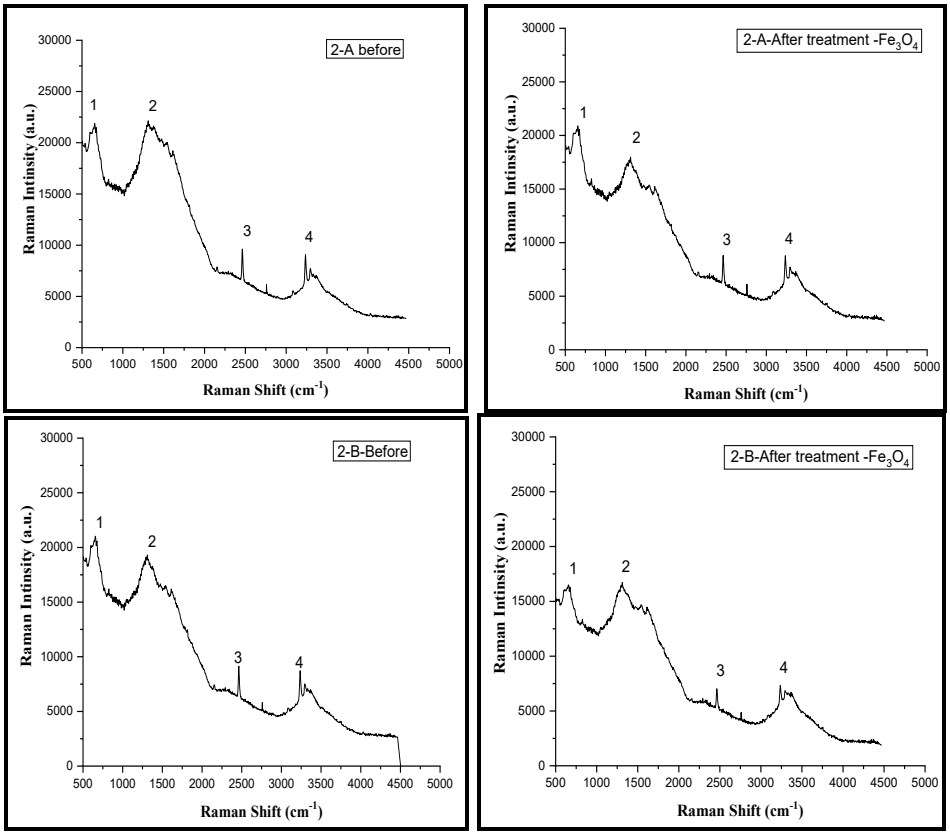

Figure 7: Raman spectra for water samples from Euphrates River before and after treatment for A- factory waste and B- sewage water

Table 5 : Results of Raman spectra for water samples from Euphrates River

Sample	Treatment	Peak number	Peak wave number (cm^{-1})	Intensity (a.u.)	Function group
A-Factory waste	Before	1	668.75	27296.86	N-H
	Before	2	1296.75	30970.95	C-O
	Before	3	2464.18	17594.60	C-H
	Before	4	3224.39	16846.58	O-H
	Fe_3O_4NPs	1	658.17	25294.80	N-H
	Fe_3O_4NPs	2	1307.33	25096	C-O
	Fe_3O_4NPs	3	2464.18	17044.58	C-H
	Fe_3O_4NPs	4	3236.29	16670.57	O-H
B -Sewage water	Before	1	658.17	27849.80	N-H
	Before	2	1307.33	27026.98	C-O
	Before	3	2464.18	18300	C-H
	Before	4	3236.29	17876.21	O-H
	Fe_3O_4NPs	1	658.17	24546.78	N-H
	Fe_3O_4NPs	2	1319.23	23094.74	C-O
	Fe_3O_4NPs	3	2464.18	11720.94	C-H
	Fe_3O_4NPs	4	3236.29	13546.49	O-H

4.4. UV-visible Spectroscopy

UV-visible absorption spectroscopy is the most widely used method at the initial stage of composition analysis of metal nanoparticles [17]. The biosynthesized Fe_3O_4NPs were analyzed using UV-visible spectroscopy, and the wavelength of the Fe_3O_4NPs suspension was measured to detect the synthesis of Fe_3O_4NPs, as shown in Figure 8. The extinction spectra of magnetite appear, where the characteristic surface plasmon absorption band is observed at the two peaks at 222 nm, and 262 nm for dark brown magnetite nanoparticles manufactured from ferric chloride with a percentage of hibiscus extract [20].

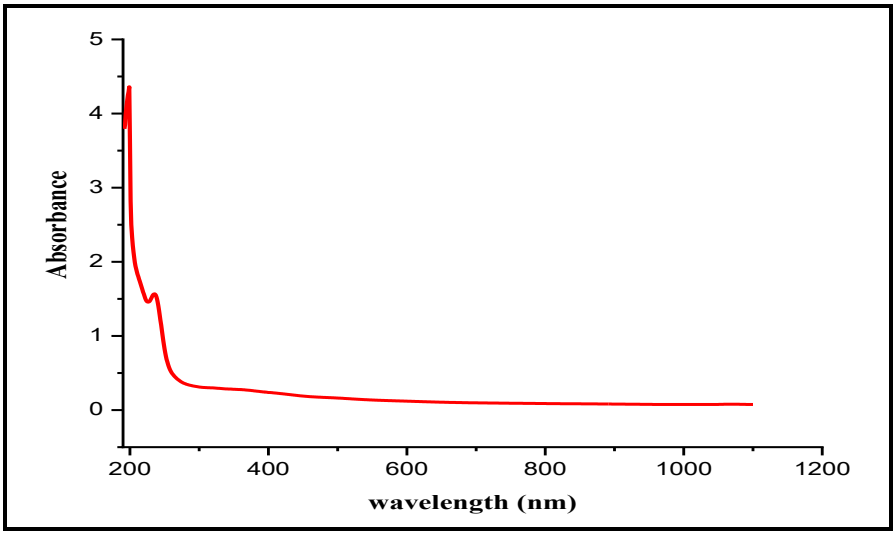

Figure 8: UV–vis absorbance spectra of Fe_3O_4NPs

The water samples from the Euphrates River at the two locations, including factory waste and sewage water, were characterized for their physical properties, as shown in Table 6. The properties were measured before and after iron oxide nanoparticles (Fe_3O_4) treatment. These properties include pH, which expresses the acidic or basic strength of water (The PH scale ranges from 0 to 14. A pH of 7 is neutral, indicating a balance between acidic and essential elements. PH values below 7 indicate increasing water acidity as PH approaches 0, while values above 7 indicate increasing water alkalinity as pH approaches 14); Total Dissolved Salts (TDS), which are a measure of the combined content of all inorganic and organic matters or salts that are found in water; Electrical Conductivity (E.C), which is the ability of water to conduct electrical current; Total Hardness (TH) of water due to the presence of calcium ions (Ca^{2+}) and magnesium ions (Mg^{2+}), two hardness types are temporary and permanent; Total Suspended Solids (TSS) of water, which include a mixture of clay, silt, some microorganisms such as plankton, and organic and inorganic materials; turbidity (Turb), which measures the relative clarity of water, where turbid water appears hazy or muddy, and turbidity is usually used to predict changes in the TSS concentration in water without accurately measuring solids [21]; and Total Aerobic Bacteria (T.P.C), which represents the bacteria that grow in the presence of oxygen [22]. The values of these properties are listed in Table 6. All the studied parameter values increased after treatment with iron oxide nanoparticles (Fe_3O_4) due to the interaction with water components, which leads to the release of iron ions in the water. These ions increase the concentration of total suspended salts, which increases the hardness of the water [23]. The turbidity and aerobic bacteria decreased after treatment, as shown in Table 6, noting that turbidity includes suspended and colloidal materials in the water such as silt, clay, organic materials, and microorganisms, Iron oxide nanoparticles are very effective for purifying water from organic and inorganic pollutants [24], especially for removing heavy metals and dyestuffs. Depending on the Iron oxide nanoparticles composite structures and

surface properties, they can function as adsorbents, photocatalysts, and coagulating agents in water remediation. They possess several advantages, such as easy separation using an external magnet, a large surface area, unique morphology, and high stability [23].

Table 6: Physical properties of water samples from Euphrates River before and after treatment.

	A- Factory waste		B- Sewage water		Sterile water
Parameter	**Before Treatment**	**Fe_3O_4NPs Treatment**	**Before Treatment**	**Fe_3O_4NPs Treatment**	
pH	6.2	6.1	7.1	7.1	6.6
TDS mg/l	802	851	946	940	76
E.C µS/CM	1235	1309	1456	1446	118
TH mg/l	540	578	600	632	50
TSS mg/l	28	39	19	28	6
Turb. NTU	19.2	12	31.4	6	0.9
T.P.C	182	15	260	12	2

The biological application employing the agar well diffusion assay showed that iron oxide nanoparticles prepared by the green synthesis method could penetrate the cell wall and effectively kill bacteria present in polluted water. Four bacterial strains usually exist in contaminated water samples: *Pseudomonas, Acinetobacter, Cholera, and Escherichia coli* [19]. The antibacterial activity of various concentrations of the synthesized Fe_3O_4 NPs is shown in Figures 9, 10, 11, and 12; Table 7 shows the inhibition values at different concentrations of the synthesized Fe_3O_4 NPs against the investigated pathogens (100% concentration means that the nanoparticles were added without diluting the concentration with deionized water). It was revealed that the different concentrations of Fe_3O_4NPs and the type of investigated pathogen caused different inhibition zones. The inhibition zone diameters increased with the increase of the Fe_3O_4 NPs concentrations. The maximum zone of inhibition was 18 mm against *Cholera*, followed by *Pseudomonas* of 13.5 mm, *Acinetobacter* of 13 mm, and *Escherichia coli* of 10 mm.

Table 7: Antibacterial activity of Fe_3O_4NPs

Antibacterial analysis (Zone of inhibition (mm))					
	Control	**12.5%**	**25%**	**50%**	**100%**
Pseudomonas	6	9	10	12	13.5
E.coli	6	6	7	8	10
Acinetobacter	6	8	10	12	13
Cholera	6	8	10	14	18

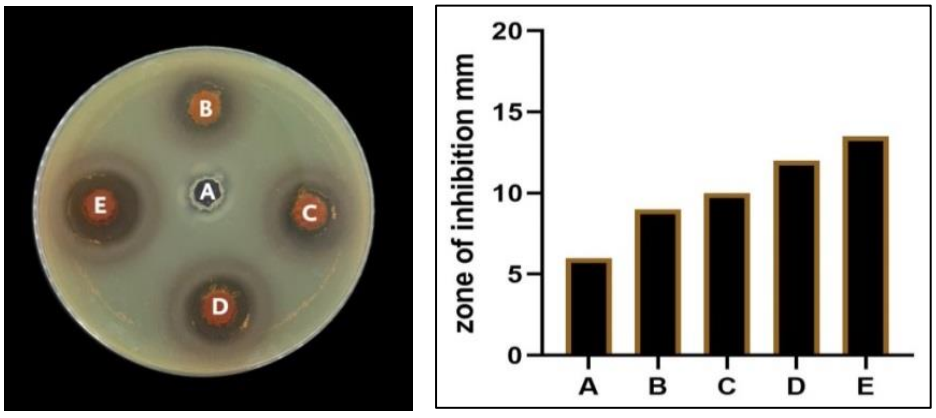

Figure 9: Antibacterial activity of Fe_3O_4 NPs against *Pseudomonas*. A, Control. B, 12.5%. C, 25%. D, 50% . E, 100%

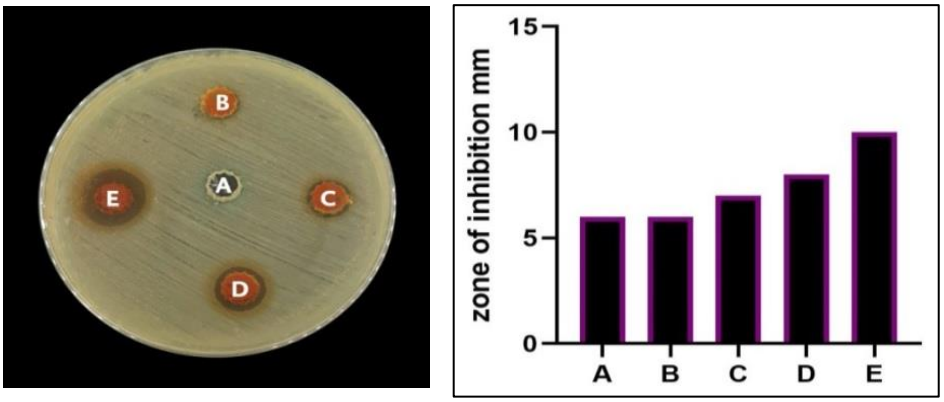

Figure 10: Antibacterial activity of Fe_3O_4 NPs against *E.coli*. A, Control. B, 12.5%. C, 25%. D, 50%. E, 100%

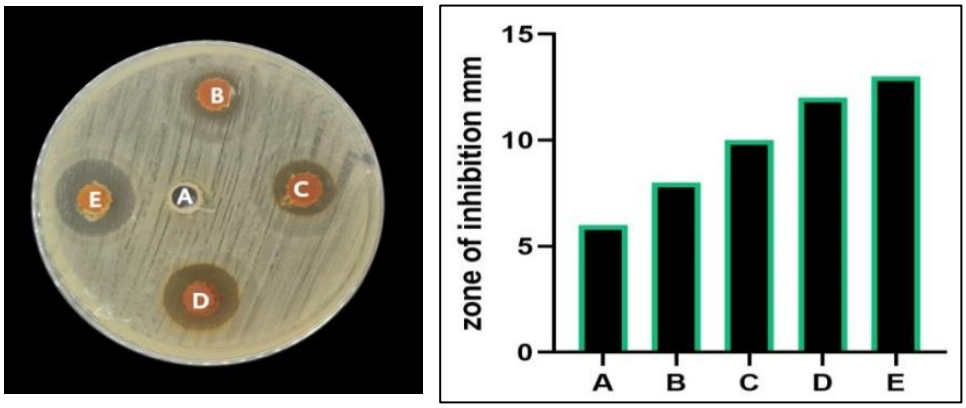

Figure 11: Antibacterial activity of Fe_3O_4 NPs against *Acinetobacter*. A, Control. B, 12.5%. C, 25%. D, 50%. E, 100%

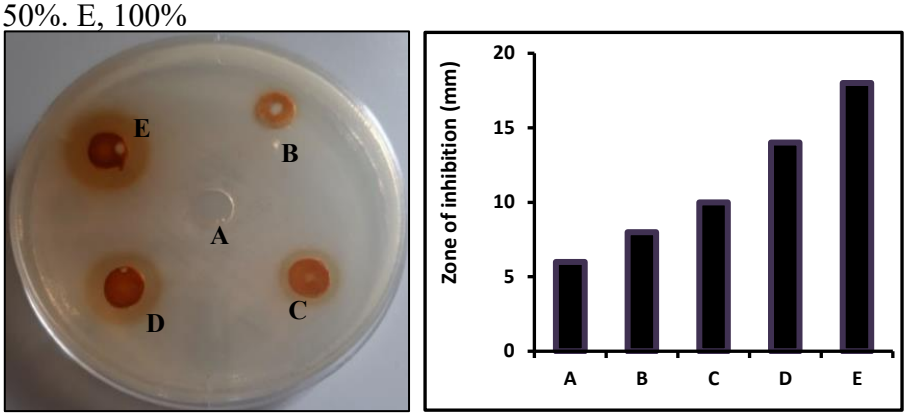

Figure 12: Antibacterial activity of Fe_3O_4NPs against *Cholera*. A, Control. B, 12.5%. C, 25%. D, 50%. E, 100%

5. Conclusion

Magnetite nanoparticles Fe_3O_4 were synthesized using the green synthesis method using hibiscus flower extract as a reductant, which is a simple, fast, and inexpensive method. The use of iron oxide nanoparticles for water pollutant treatment was discussed. Fe_3O_4-based sorbents are promising for wastewater treatment due to their high adsorption capacity. Being very stable during the adsorption process, Fe_3O_4 -based adsorbents have shown promise in eliminating pollutants in wastewater; compared to other adsorbents and sorbents, due to stability, efficiency, and selectivity towards pollutants. The treatment by Fe_3O_4 NPs showed that turbidity and total aerobic bacteria (which play an essential role in water pollution) decreased

after treatment. Its antibacterial ability against gram-negative bacterial strains is also common in contaminated water (*Pseudomonas, Acinetobacter, Cholera,* and *Escherichia coli*). The inhibition area is strongly affected by Fe_3O_4NP concentration, increasing with concentration increase. It also depends on the type of bacteria based on the ability of the Fe_3O_4NPs to penetrate the bacterial cytoplasmic membrane.

6. **Acknowledgements**

The authors would like to thank Mustansiryiah University – Iraq for their logistic support, (www.uomustansiriyah.edu.iq).

Reference

[1] K. E. Drexled, "Engines of creation: the coming era of nanotechnology," Anchor Press, 1986.

[2] A. Bouafia, S. E. Laouini, M. L. Tedjani, G. A. M. Ali, and A. Barhoum, "Green biosynthesis and physicochemical characterization of Fe_3O_4 nanoparticles using Punica granatum L. fruit peel extract for optoelectronic applications," *Text. Res. J.*, vol. 92, no. 15–16, pp. 2685–2696, 2022.

[3] M. Mahnaz, M. B. Ahmad, M. J. Haron, F. Namvar, B. N. M. Z. A. Rahman, and J. Amin, "Synthesis, surface modification and characterisation of biocompatible magnetic iron oxide nanoparticles for biomedical applications," *Molecules*, vol. 18, no. 7, pp. 7533–7548, 2013.

[4] A. S. Teja and P.-Y. Koh, "Synthesis, properties, and applications of magnetic iron oxide nanoparticles," *Prog. Cryst. growth Charact. Mater.*, vol. 55, no. 1–2, pp. 22–45, 2009.

[5] S. N. Mazhir, N. F. Majeed, E. M. Abbas, and S. A. Qasim, "Synthesis of Green Zno/Fe_3O_4 Nanocomposite by Microplasma Jet and Anti-Bacterial Agent," *Iraqi J. Sci.*, vol. 64, no. 12, pp. 6215–6225, 2023.

[6] I. O. Sule, O. C. Adekunle, I. O. Adebesin, Z. B. Abdulsalam, O. I. Oladunjoye, and M. Muhammed, "Water Quality Assessment, Antibiotic Resistance and Plasmid Profiles of Bacteria Isolated from Asa River, Ilorin, Nigeria," *Iraqi J. Sci.*, vol. 64, no. 12, pp. 6148–6157, 2023.

[7] J. N. Hamza, A. M. S. Ameen, and T. A. Mohammad "The Effects of Intake Water Quality and Filtration Unit Performance on the Efficiency of the Al-Rasheed Water Treatment Plant in Baghdad, Iraq," *Iraqi J. Sci.*, vol. 64, no. 12, pp. 6158–6174, 2023.

[8] H. H. Bahjat, R. A. Ismail, G. M. Sulaiman, and M. S. Jabir, "Magnetic field-assisted laser ablation of titanium dioxide nanoparticles in water for anti-bacterial applications," *J. Inorg. Organomet. Polym. Mater.*, vol. 31, no. 9, pp. 3649–3656, 2021.

[9] K. S. Khashan, F. A. Abdulameer, M. S. Jabir, A. A. Hadi, and G. M. Sulaiman, "Anticancer activity and toxicity of carbon nanoparticles produced by pulsed laser ablation of graphite in water," *Adv. Nat. Sci. Nanosci. Nanotechnol.*, vol. 11, no. 3, p. 35010, 2020.

[10] K. S. Khashan, B. A. Badr, G. M. Sulaiman, M. S. Jabir, and S. A. Hussain, "Antibacterial activity of Zinc Oxide nanostructured materials synthesis by laser ablation method," *Journal of physics: conference series*, IOP Publishing, p. 12040, 2021.

[11] M. A. Jihad, F. T. M. Noori, M. S. Jabir, S. Albukhaty, F. A. AlMalki, and A. A. Alyamani, "Polyethylene glycol functionalized graphene oxide nanoparticles loaded with nigella sativa extract: a smart antibacterial therapeutic drug delivery system," *Molecules*, vol. 26, no. 11, p. 3067, 2021.

[12] M. K. A. Mohammed, M. R. Mohammad, M. S. Jabir, and D. S. Ahmed, "Functionalization, characterization, and antibacterial activity of single wall and multi wall carbon nanotubes," in *IOP Conference Series: Materials Science and Engineering*, IOP Publishing, p. 12028,2020.

[13] M. Yusefi, K. Shameli, R. R. Ali, S.-W. Pang, and S.-Y. Teow, "Evaluating anticancer activity of plant-mediated synthesized iron oxide nanoparticles using Punica granatum fruit peel extract," *J. Mol. Struct.*, vol. 1204, p. 127539, 2020.

[14] I. Zahra, K. Shameli, M. Miyake, H. Hara, S. E. B. Mohamad, K. Kalantari, S. Husnaa M. Taib, and E. Rasouli., "Cytotoxicity assay of plant-mediated synthesized iron oxide nanoparticles using Juglans regia green husk extract," *Arab. J. Chem.*, vol. 13, no. 1, pp. 2011–2023, 2020.

[15] S. Gnanasekar, V. Logeshwaran, S. Sarathbabu, P. K. Jha, M. Jeyaraj, C. Rajkuberan, N. Senthilkumar, and S. Sivaramakrishnan, "Green synthesis of magnetic Fe3O4 nanoparticles using Couroupita guianensis Aubl. fruit extract for their antibacterial and cytotoxicity activities," *Artif. cells, nanomedicine, Biotechnol.*, vol. 46, no. 3, pp. 589–598, 2018.

[16] M. Yusefi , K. Shameli, O. S. Yee, S.-Y. Teow, Z. Hedayatnasab, H. Jahangirian, T. J. Webster, and K. Kuča, "Green synthesis of Fe3O4 nanoparticles stabilized by a Garcinia mangostana fruit peel extract for hyperthermia and anticancer activities," *Int. J. Nanomedicine*, vol. 16, pp. 2515–2532, 2021.

[17] A. Farida, S. Konnova, M. Kryuchkova, S. Batasheva, K. Mazurova, A. Vikulina, D.Volodkin, and E. Rozhina., "Comparative characterization of iron and silver nanoparticles: extract-stabilized and classical synthesis methods," *Int. J. Mol. Sci.*, vol. 24, no. 11, p. 9274, 2023.

[18] I. Durickovic and M. Marchetti, "Raman spectroscopy as polyvalent alternative for water pollution detection," *IET Sci. Meas. Technol.*, vol. 8, no. 3, pp. 122–128, 2014.

[19] S. S. Mohammed, A. M. Awadelgied, S. saad El Wakeel, and A. A. Mohamed, "The Ability of Raman Spectroscopy to Detect Surface Water Pollution in Northern Sudan," *International Journal of Trend in Scientific Research and Development*, vol. *3,* no.3, pp.1805 -1811, 2019.

[20] M. D. Nguyen, H.-V. Tran, S. Xu, and T. R. Lee, "Fe3O4 nanoparticles: structures, synthesis, magnetic properties, surface functionalization, and emerging applications," *Appl. Sci.*, vol. 11, no. 23, p. 11301, 2021.

[21] M. W. Jumaa and R. S. Abdulqader, "Evaluation of Drinking Water Quality Index in Kirkuk City, *Iraq Central Asian Journal of Medical and Natural Science*, vol. 5, no. 3, pp. 815-823, 2024.

[22] H. Umeshappa, A. Shetty, K. Kavatagi, G. K. Vivek, N. Vaibhav, and I. Mohammed, "Microbiological profile of aerobic and anaerobic bacteria and its clinical significance in antibiotic sensitivity of odontogenic space infection: A prospective study of 5 years," *Natl. J. Maxillofac. Surg.*, vol. 12, no. 3, pp. 372–379, 2021.

[23] M. Sharma, P. Kalita, K. K. Senapati, and A. Garg, "Study on magnetic materials for removal of water pollutants," Emerging Pollutants - Some Strategies for the Quality Preservation of Our Environment, Sonia Soloneski and Marcelo L. Larramendy(Eds), IntechOpen, pp. 61–78, 2018.

[24] B. E. Keshta, Ali H. Gemeay, Durgesh Kumar Sinha, Safya Elsharkawy, Fathy Hassan, Nidhi Rai, and Charu Arora, "State of the art on the magnetic iron oxide Nanoparticles: Synthesis, Functionalization, and applications in wastewater treatment," *Results Chem.*, vol. 7, p. 101388, 2024.